PHYSICAL REVIEW D **71,** 091106(R) (2005)

Measurements of branching fractions and CP asymmetries in $B \to \eta h$ decays

P. Chang,[24] K. Abe,[7] K. Abe,[39] H. Aihara,[41] M. Akatsu,[19] Y. Asano,[44] T. Aushev,[10] A. M. Bakich,[36] V. Balagura,[10] Y. Ban,[31] S. Banerjee,[37] I. Bedny,[1] U. Bitenc,[11] I. Bizjak,[11] S. Blyth,[24] A. Bondar,[1] A. Bozek,[25] M. Bračko,[7,17,11] J. Brodzicka,[25] T. E. Browder,[6] Y. Chao,[24] A. Chen,[21] K.-F. Chen,[24] B. G. Cheon,[3] R. Chistov,[10] S.-K. Choi,[5] Y. Choi,[35] A. Chuvikov,[32] S. Cole,[36] J. Dalseno,[18] M. Danilov,[10] M. Dash,[45] J. Dragic,[18] A. Drutskoy,[4] S. Eidelman,[1] V. Eiges,[10] S. Fratina,[11] N. Gabyshev,[1] A. Garmash,[32] T. Gershon,[7] G. Gokhroo,[37] R. Guo,[22] J. Haba,[7] K. Hayasaka,[19] H. Hayashii,[20] M. Hazumi,[7] T. Hokuue,[19] Y. Hoshi,[39] S. Hou,[21] W.-S. Hou,[24] Y. B. Hsiung,[24] H.-C. Huang,[24] T. Iijima,[19] A. Imoto,[20] K. Inami,[19] A. Ishikawa,[7] R. Itoh,[7] M. Iwasaki,[41] Y. Iwasaki,[7] J. H. Kang,[46] J. S. Kang,[13] P. Kapusta,[25] N. Katayama,[7] H. Kawai,[2] T. Kawasaki,[27] H. R. Khan,[42] H. Kichimi,[7] H. J. Kim,[14] J. H. Kim,[35] S. K. Kim,[34] S. M. Kim,[35] P. Koppenburg,[7] S. Korpar,[17,11] P. Križan,[16,11] P. Krokovny,[1] R. Kulasiri,[4] C. C. Kuo,[21] Y.-J. Kwon,[46] S. E. Lee,[34] S. H. Lee,[34] T. Lesiak,[25] J. Li,[33] S.-W. Lin,[24] D. Liventsev,[10] G. Majumder,[37] F. Mandl,[9] T. Matsumoto,[43] W. Mitaroff,[9] K. Miyabayashi,[20] H. Miyake,[29] H. Miyata,[27] R. Mizuk,[10] D. Mohapatra,[45] T. Mori,[42] T. Nagamine,[40] Y. Nagasaka,[8] E. Nakano,[28] M. Nakao,[7] S. Nishida,[7] S. Ogawa,[38] T. Ohshima,[19] T. Okabe,[19] S. Okuno,[12] S. L. Olsen,[6] W. Ostrowicz,[25] H. Ozaki,[7] P. Pakhlov,[10] C. W. Park,[35] H. Park,[14] N. Parslow,[36] R. Pestotnik,[11] L. E. Piilonen,[45] M. Rozanska,[25] H. Sagawa,[7] Y. Sakai,[7] T. Schietinger,[15] O. Schneider,[15] P. Schönmeier,[40] J. Schümann,[24] A. J. Schwartz,[4] K. Senyo,[19] H. Shibuya,[38] J. B. Singh,[30] A. Somov,[4] N. Soni,[30] R. Stamen,[7] S. Stanič,[44] M. Starič,[11] K. Sumisawa,[29] T. Sumiyoshi,[43] O. Tajima,[7] F. Takasaki,[7] N. Tamura,[27] M. Tanaka,[7] Y. Teramoto,[28] X. C. Tian,[31] S. Uehara,[7] T. Uglov,[10] K. Ueno,[24] S. Uno,[7] Y. Ushiroda,[7] G. Varner,[6] K. E. Varvell,[36] S. Villa,[15] C. C. Wang,[24] C. H. Wang,[23] M.-Z. Wang,[24] A. Yamaguchi,[40] H. Yamamoto,[40] Y. Yamashita,[26] M. Yamauchi,[7] Heyoung Yang,[34] J. Ying,[31] J. Zhang,[7] L. M. Zhang,[33] Z. P. Zhang,[33] V. Zhilich,[1] and D. Žontar[16,11]

(Belle Collaboration)

[1]*Budker Institute of Nuclear Physics, Novosibirsk*
[2]*Chiba University, Chiba*
[3]*Chonnam National University, Kwangju*
[4]*University of Cincinnati, Cincinnati, Ohio 45221, USA*
[5]*Gyeongsang National University, Chinju*
[6]*University of Hawaii, Honolulu, Hawaii 96822, USA*
[7]*High Energy Accelerator Research Organization (KEK), Tsukuba*
[8]*Hiroshima Institute of Technology, Hiroshima*
[9]*Institute of High Energy Physics, Vienna*
[10]*Institute for Theoretical and Experimental Physics, Moscow*
[11]*J. Stefan Institute, Ljubljana*
[12]*Kanagawa University, Yokohama*
[13]*Korea University, Seoul*
[14]*Kyungpook National University, Taegu*
[15]*Swiss Federal Institute of Technology of Lausanne, EPFL, Lausanne*
[16]*University of Ljubljana, Ljubljana*
[17]*University of Maribor, Maribor*
[18]*University of Melbourne, Victoria*
[19]*Nagoya University, Nagoya*
[20]*Nara Women's University, Nara*
[21]*National Central University, Chung-li*
[22]*National Kaohsiung Normal University, Kaohsiung*
[23]*National United University, Miao Li*
[24]*Department of Physics, National Taiwan University, Taipei*
[25]*H. Niewodniczanski Institute of Nuclear Physics, Krakow*
[26]*Nihon Dental College, Niigata*
[27]*Niigata University, Niigata*
[28]*Osaka City University, Osaka*
[29]*Osaka University, Osaka*
[30]*Panjab University, Chandigarh*
[31]*Peking University, Beijing*
[32]*Princeton University, Princeton, New Jersey 08545, USA*

[33]*University of Science and Technology of China, Hefei*
[34]*Seoul National University, Seoul*
[35]*Sungkyunkwan University, Suwon*
[36]*University of Sydney, Sydney NSW*
[37]*Tata Institute of Fundamental Research, Bombay*
[38]*Toho University, Funabashi*
[39]*Tohoku Gakuin University, Tagajo*
[40]*Tohoku University, Sendai*
[41]*Department of Physics, University of Tokyo, Tokyo*
[42]*Tokyo Institute of Technology, Tokyo*
[43]*Tokyo Metropolitan University, Tokyo*
[44]*University of Tsukuba, Tsukuba*
[45]*Virginia Polytechnic Institute and State University, Blacksburg, Virginia 24061, USA*
[46]*Yonsei University, Seoul*

(Received 14 December 2004; published 23 May 2005)

We report measurements of B to pseudoscalar-pseudoscalar decays with at least one η meson in the final state using 140 fb^{-1} of data collected by the Belle detector at KEKB e^+e^- collider. We observe the decay $B^+ \to \eta\pi^+$ and find evidence of $B^+ \to \eta K^+$; the measured branching fractions are $\mathcal{B}(B^+ \to \eta\pi^+) = (4.8^{+0.8}_{-0.7}(\text{stat}) \pm 0.3(\text{sys})) \times 10^{-6}$ and $\mathcal{B}(B^+ \to \eta K^+) = (2.1 \pm 0.6(\text{stat}) \pm 0.2(\text{sys})) \times 10^{-6}$. Their corresponding CP violating asymmetries are measured to be $0.07 \pm 0.15(\text{stat}) \pm 0.03(\text{sys})$ for $\eta\pi^\pm$ and $-0.49 \pm 0.31(\text{stat}) \pm 0.07(\text{sys})$ for $\eta K^\pm$. No significant signals are found for neutral $B \to \eta h$ decays. We report the following upper limits on branching fractions at the 90% confidence level: $\mathcal{B}(B^0 \to \eta K^0) < 2.0 \times 10^{-6}$, $\mathcal{B}(B^0 \to \eta\pi^0) < 2.5 \times 10^{-6}$ and $\mathcal{B}(B^0 \to \eta\eta) < 2.0 \times 10^{-6}$.

DOI: 10.1103/PhysRevD.71.091106 PACS numbers: 13.25.Hw, 11.30.Er, 12.15.Hh

Charmless B decays provide a rich sample to understand B decay dynamics and to search for CP violation. An unexpectedly large $B \to \eta' K$ branching fraction [1,2] has stimulated much theoretical interest. It was suggested even before the $\eta' K$ measurement that two $b \to s$ penguin amplitudes are constructive in $B \to \eta' K$ decays but destructive in $B \to \eta K$ [3]. The situation is reversed for $B \to \eta' K^*$ and $B \to \eta K^*$ decays. Experimental results have more or less confirmed this picture; however, precise measurements of branching fractions are needed to quantitatively understand the contribution of each diagram. It was also pointed out that in the ηK mode the suppressed penguin amplitudes may interfere with the CKM suppressed $b \to u$ (tree) amplitude and result in direct CP violation [4]. The penguin-tree interference may also be large in $B^+ \to \eta'\pi^+$ [5] and $B^+ \to \eta\pi^+$ decays; however, theoretical expectations for the partial rate asymmetry (A_{CP}) can be either positive or negative [4,6]. Recently, the BABAR Collaboration has reported large negative A_{CP} values in both ηK^+ and $\eta\pi^+$, which are $\sim 2\sigma$ away from zero [7]. However, more data are needed to verify these large CP violating asymmetries. Furthermore, branching fractions and partial rate asymmetries in charmless B decays can be used to understand the tree and penguin contributions and provide constraints on the third unitarity triangle angle ϕ_3 [8].

In this paper, we report measurements of branching fractions and partial rate asymmetries for $B \to \eta h$ decays, where h could be a K, π or η meson. The partial rate asymmetry is measured for the charged B decays and defined to be:

$$\mathcal{A}_{CP} = \frac{N(B^- \to \eta h^-) - N(B^+ \to \eta h^+)}{N(B^- \to \eta h^-) + N(B^+ \to \eta h^+)},$$

where $N(B^-)$ is the yield for the $B^- \to \eta h^-$ decay and $N(B^+)$ denotes that of the charge conjugate mode. The data sample consists of 152×10^6 $B\overline{B}$pairs (140 fb^{-1}) collected with the Belle detector at the KEKB e^+e^- asymmetric-energy (3.5 on 8 GeV) collider [9] operating at the $\Upsilon(4S)$ resonance.

The Belle detector is a large-solid-angle magnetic spectrometer that consists of a three-layer silicon vertex detector (SVD), a 50-layer central drift chamber (CDC), an array of aerogel threshold Čerenkov counters (ACC), a barrel-like arrangement of time-of-flight scintillation counters (TOF), and an electromagnetic calorimeter (ECL) comprised of CsI(Tl) crystals located inside a superconducting solenoid coil that provides a 1.5 T magnetic field. An iron flux-return located outside of the coil is instrumented to detect K_L^0 mesons and to identify muons (KLM). The detector is described in detail elsewhere [10].

Two η decay channels are considered in this analysis: $\eta \to \gamma\gamma$ ($\eta_{\gamma\gamma}$) and $\eta \to \pi^+\pi^-\pi^0$ ($\eta_{3\pi}$). In the $\eta_{\gamma\gamma}$ reconstruction, each photon is required to have a minimum laboratory energy of 50 MeV and the energy asymmetry, defined as the absolute value of the energy difference in the laboratory frame between the two photons divided by their energy sum, must be less than 0.9. Furthermore, we remove η candidates if either one of the daughter photons can pair with any other photon to form a π^0 candidate. Candidate

*on leave from Nova Gorica Polytechnic, Nova Gorica

$\eta_{3\pi}$ mesons are reconstructed by combining a π^0 with a pair of oppositely charged tracks that originate from the interaction point (IP). In order to maintain a high reconstruction efficiency, no $K-\pi$ separation requirement is applied to reconstruct $\eta_{3\pi}$. We make the following requirements for the invariant mass on the η candidates: $516\ \mathrm{MeV}/c^2 < M_{\gamma\gamma} < 569\ \mathrm{MeV}/c^2$ for $\eta_{\gamma\gamma}$ and $539\ \mathrm{MeV}/c^2 < M_{3\pi} < 556\ \mathrm{MeV}/c^2$ for $\eta_{3\pi}$. After the selection of each candidate, an η mass constraint is implemented by readjusting the momentum vectors of the daughter particles.

Candidate neutral pions are selected by requiring the two-photon invariant mass to be in the mass window between $115\ \mathrm{MeV}/c^2$ and $152\ \mathrm{MeV}/c^2$. The momentum vector of each photon is then readjusted to constrain the mass of the photon pair to be the nominal π^0 mass. To reduce the low energy photon background, each photon is required to have a minimum energy of 50 MeV and the π^0 momentum must be above $250\ \mathrm{MeV}/c$ in the laboratory frame. Charged tracks are required to come from the IP. Charged kaons and pions that form B candidates with η mesons are identified by combining information from the CDC (dE/dx), the TOF and the ACC to form a $K(\pi)$ likelihood $L_K(L_\pi)$. Discrimination between kaons and pions is achieved through the likelihood ratio $L_K/(L_\pi + L_K)$. Charged tracks with likelihood ratios greater than 0.6 are regarded as kaons, and less than 0.4 as pions. The typical kaon and pion identification efficiencies for $2.5\ \mathrm{GeV}/c$ tracks are $(85.0 \pm 0.2)\%$ and $(89.3 \pm 0.2)\%$, respectively. The corresponding rate for pions to be misidentified as kaons is $(7.3 \pm 0.2)\%$ while the rate for kaons to be misidentified as pions is $(10.6 \pm 0.2)\%$. Furthermore, charged tracks that are positively identified as electrons or muons are rejected. K^0_S candidates are reconstructed from pairs of oppositely charged tracks with invariant mass ($M_{\pi\pi}$) between 480 to $516\ \mathrm{MeV}/c^2$. Each candidate must have a displaced vertex with a flight direction consistent with a K^0_S originating from the IP.

Candidate B mesons are identified using the beam constrained mass, $M_{\mathrm{bc}} = \sqrt{E^2_{\mathrm{beam}} - P^2_B}$, and the energy difference, $\Delta E = E_B - E_{\mathrm{beam}}$, where E_{beam} is the run-dependent beam energy in the $\Upsilon(4S)$ rest frame and is determined from $B \to D^{(*)}\pi$ events, and P_B and E_B are the momentum and energy of the B candidate in the $\Upsilon(4S)$ rest frame. The resolutions on M_{bc} and ΔE are around $3\ \mathrm{MeV}/c^2$ and $\sim$20–30 MeV, respectively. Events with $M_{\mathrm{bc}} > 5.2\ \mathrm{GeV}/c^2$ and $|\Delta E| < 0.3$ GeV are selected for the analysis.

The dominant background comes from the $e^+e^- \to q\bar{q}$ continuum, where $q = u, d, s$ or c. To distinguish signal from the jetlike continuum background, event shape variables and the B flavor tagging information are employed. We form a Fisher discriminant [11] from seven variables that quantify event topology. The Fisher variables include the angle θ_T between the thrust axis [12] of the B candidate and the thrust axis of the rest of the event, five modified Fox-Wolfram moments [13], and a measure of the momentum transverse to the event thrust axis ($S_\perp$) [14]. The probability density functions (PDF) for this discriminant and $\cos\theta_B$, where θ_B is the angle between the B flight direction and the beam direction in the $\Upsilon(4S)$ rest frame, are obtained using events in signal Monte Carlo (MC) and data with $M_{\mathrm{bc}} < 5.26\ \mathrm{GeV}/c^2$ for signal and $q\bar{q}$ background, respectively. These two variables are then combined to form a likelihood ratio $\mathcal{R} = \mathcal{L}_s/(\mathcal{L}_s + \mathcal{L}_{q\bar{q}})$, where $\mathcal{L}_{s(q\bar{q})}$ is the product of signal ($q\bar{q}$) probability densities.

Additional background discrimination is provided by the quality of the$B$ flavor tagging of the accompanying B meson. We use the standard Belle B tagging package [15], which gives two outputs: a discrete variable (q) indicating the B flavor and a dilution factor (r) ranging from zero for no flavor information to unity for unambiguous flavor assignment. We divide the data into six r regions. Continuum suppression is achieved by applying a mode dependent requirement on $\mathcal{R}$ for events in each r region based on $N^{\mathrm{exp}}_s/\sqrt{N^{\mathrm{exp}}_s + N^{\mathrm{exp}}_{q\bar{q}}}$, where N^{exp}_s is the expected signal from MC and $N^{\mathrm{exp}}_{q\bar{q}}$ denotes the number of background events estimated from data. This $\mathcal{R}$ requirement retains 58–86% of the signal while reducing 96–82% of the background. From MC all other backgrounds are found to be negligible except for the $\eta K^+ \leftrightarrow \eta\pi^+$ reflection, due to $K^+ \leftrightarrow \pi^+$ misidentification, and the $\eta K^*(892)(\eta\rho(770))$ feed-down to the $\eta K(\eta\pi)$ modes. We include these two components in the fit used to extract the signal.

The signal yields and branching fractions are obtained using an extended unbinned maximum-likelihood (ML) fit with input variables M_{bc} and ΔE. The likelihood is defined as:

$$\mathcal{L} = \exp(-\sum_j N_j)\prod_i^N\Big[\sum N_j P_j(M_{\mathrm{bc}i}, \Delta E_i)\Big],$$

where N_j is the yield of category j (signal, continuum background, reflection, $\eta K^*/\eta\rho$), $P_j(M_{\mathrm{bc}i}, \Delta E_i)$ is the probability density for the ith event and N is the total number of events. The PDFs for the signal, the reflection background and the $\eta K^*/\eta\rho$ feed-down are modeled with two-dimensional M_{bc}-ΔE smooth functions obtained using MC. The signal peak positions and resolutions in M_{bc} and ΔE are adjusted according to the data-MC differences using large control samples of $B \to D\pi$ and $\overline{D}^0 \to K^+\pi^-\pi^0/\pi^0\pi^0$ decays. The continuum background in ΔE is described by a first or second order polynomial while the M_{bc} distribution is parameterized by an ARGUS function, $f(x) = x\sqrt{1-x^2}\exp[-\xi(1-x^2)]$, where x is M_{bc} divided by half of the total center of mass energy [16]. Thus the continuum PDF is the product of an ARGUS function and a polynomial, where ξ and the

coefficients of the polynomial are free parameters. Since $B \to \eta K^*$ branching fractions are well measured ($\sim 20 \times 10^{-6}$) [1,17], their feed-down to the ηK modes are fixed from MC in the likelihood fit. Since the decay $B^+ \to \eta \rho^+$ is experimentally poorly constrained, the amount of this background in the $\eta\pi$ modes is allowed to float in the fit. In the charged B modes, the normalizations of the reflections are fixed to expectations based on the $B^+ \to \eta K^+$ and $B^+ \to \eta \pi^+$ branching fractions and $K^+ \leftrightarrow \pi^+$ fake rates, measured using $\overline{D}^0 \to K^+\pi^-$ data. The reflection yield is first estimated with the assumed ηK^+ and $\eta\pi^+$ branching fractions and is then recalculated according to our measured branching fractions. No $B\overline{B}$ contributions are included for the $B^0 \to \eta\eta$ mode.

In Table I we show the measured branching fractions for each decay mode as well as other quantities associated with the measurements. The efficiency for each mode is determined using MC simulation and corrected for the discrepancy between data and MC using the control samples. The only discrepancy we find is the performance of particle identification, which results in a 4.3% correction for the $\eta\pi^+$ mode and 1.7% for $B \to \eta K^+$. The combined branching fraction of the two η decay modes is obtained from a simultaneous likelihood fit to all the subsamples with a common branching fraction. Systematic uncertainties in the fit due to the uncertainties in the signal PDFs are estimated by performing the fit after varying their peak positions and resolutions by 1 standard deviation. The ηK^+ reflection in the $\eta\pi^+$ sample is $(3.1 \pm 1.8)/(1.1 \pm 1.0)$ events for the $\eta_{\gamma\gamma}/\eta_{3\pi}$ mode, while the $\eta\pi^+$ reflection to the ηK^+ candidates is $(4.1 \pm 2.0)/(1.7 \pm 1.3)$ events for $\eta_{\gamma\gamma}/\eta_{3\pi}$. The reflection yields are varied by 1 standard deviation in the fit to obtain the corresponding systematic uncertainties. In the ηK modes, we also vary the expected ηK^* feed-down by 1 standard deviation to check the yield difference. The quadratic sum of the deviations from the central value gives the systematic uncertainty in the fit, which ranges from 3% to 6%. For each systematic check, the statistical significance is taken as the square root of the difference between the value of $-2\ln\mathcal{L}$ for zero signal yield and the best-fit value. We regard the smallest value as our significance including the systematic uncertainty. The number of B^+B^- and $B^0\overline{B}^0$ pairs are assumed to be equal.

The performance of the $\mathcal{R}$ requirement is studied by checking the data-MC efficiency ratio using the $B^+ \to \overline{D}^0\pi^+$ control sample. The obtained error is 2.4–3.5%. The systematic errors on the charged track reconstruction are estimated to be around 1% per track using partially reconstructed D^* events, and verified by comparing the ratio of $\eta \to \pi^+\pi^-\pi^0$ to $\eta \to \gamma\gamma$ in data with MC expectations. The π^0 and $\eta_{\gamma\gamma}$ reconstruction efficiency is verified by comparing the π^0 decay angular distribution with the MC prediction, and by measuring the ratio of the branching fractions for the two η decay channels: $\eta \to \gamma\gamma$ and $\eta \to \pi^0\pi^0\pi^0$. We assign a 3.5% error for the π^0 and $\eta_{\gamma\gamma}$ reconstruction. The K^0_S reconstruction is verified by comparing the ratio of $D^+ \to K^0_S\pi^+$ and $D^+ \to K^-\pi^+\pi^+$

TABLE I. Detection efficiency (ϵ), product of daughter branching fractions ($\prod \mathcal{B}_i$), yield, significance (Sig.), measured branching fraction ($\mathcal{B}$), the 90% C.L. upper limit (UL) and A_{CP} for the $B \to \eta h$ decays. The first errors in columns 4, 6 and 8 are statistical and the second errors are systematic.

Mode	ϵ(%)	$\prod \mathcal{B}_i$(%)	Yield	Sig.	$\mathcal{B}(10^{-6})$	UL(10^{-6})	A_{CP}
$B^+ \to \eta\pi^+$				8.0	$4.8 \pm 0.7 \pm 0.3$		$0.07 \pm 0.15 \pm 0.03$
$\eta_{\gamma\gamma}\pi^+$	23.3	39.4	$73.4^{+13.5}_{-12.7} \pm 2.0$	7.0	$5.3^{+1.0}_{-0.9} \pm 0.3$		$0.11 \pm 0.17 \pm 0.03$
$\eta_{3\pi}\pi^+$	14.8	22.6	$19.6^{+7.0}_{-6.1} \pm 0.7$	3.9	$3.8^{+1.4}_{-1.2} \pm 0.3$		$-0.11^{+0.35+0.04}_{-0.33-0.05}$
$B^+ \to \eta K^+$				3.7	$2.1 \pm 0.6 \pm 0.2$		$-0.49 \pm 0.31 \pm 0.07$
$\eta_{\gamma\gamma}K^+$	21.1	39.4	$28.0^{+10.0}_{-9.1} \pm 1.6$	3.3	$2.2^{+0.8}_{-0.7} \pm 0.2$		$-0.45^{+0.35}_{-0.31} \pm 0.07$
$\eta_{3\pi}K^+$	13.8	22.6	$7.4^{+5.4}_{-4.5} \pm 0.5$	1.7	$1.5^{+1.1}_{-0.9} \pm 0.2$		$-0.78^{+1.03+0.11}_{-0.76-0.12}$
$B^0 \to \eta K^0$				0.4	$0.3^{+0.9}_{-0.7} \pm 0.1$	<2.0	
$\eta_{\gamma\gamma}K^0$	22.9	13.6	$-1.9^{+4.3}_{-3.1} \pm 0.3$	–	$-0.4^{+0.9}_{-0.7} \pm 0.1$		
$\eta_{3\pi}K^0$	12.2	7.8	$3.5^{+3.6}_{-2.7} \pm 0.2$	1.3	$2.4^{+2.5}_{-1.9} \pm \pm 0.3$		
$B^0 \to \eta\pi^0$				1.8	$1.2 \pm 0.7 \pm 0.1$	<2.5	
$\eta_{\gamma\gamma}\pi^0$	17.0	39.0	$18.2^{+8.9+0.8}_{-8.0-0.7}$	2.4	$1.8^{+0.9}_{-0.8} \pm 0.2$		
$\eta_{3\pi}\pi^0$	11.2	22.3	$-3.0^{+5.0}_{-4.0} \pm 0.3$	–	$-0.8^{+1.3}_{-0.8} \pm 0.1$		
$B^0 \to \eta\eta$				1.1	$0.7^{+0.7}_{-0.6} \pm 0.1$	<2.0	
$\eta_{\gamma\gamma}\eta_{\gamma\gamma}$	16.9	15.5	$-1.5^{+2.7}_{-1.6} \pm 0.1$	–	$-0.4^{+0.7}_{-0.4} \pm 0.0$		
$\eta_{\gamma\gamma}\eta_{3\pi}$	11.3	17.8	$7.3^{+4.5}_{-4.0} \pm 0.2$	2.2	$2.3^{+1.4}_{-1.2} \pm 0.2$		
$\eta_{3\pi}\eta_{3\pi}$	7.7	5.1	$0.3^{+2.0}_{-1.2} \pm 0.1$	0.2	$0.5^{+3.1}_{-1.9} \pm 0.1$		

yields. The resulting K_S^0 detection systematic error is 4.4%. The uncertainty in the number of $B\overline{B}$ events is 1%. The final systematic error is obtained by first summing all correlated errors linearly and then quadratically summing the uncorrelated errors.

Figure 1 shows the $M_{\rm bc}$ and ΔE projections after requiring events to satisfy -0.10 GeV $< \Delta E < 0.08$ GeV (-0.15 GeV $< \Delta E < 0.10$ GeV for the $\eta_{\gamma\gamma}$ and $\eta\pi^0$ modes) and $M_{\rm bc} > 5.27$ GeV$/c^2$, respectively. No significant signals are observed for the neutral B meson modes; for these modes we set branching fraction upper limits at the 90% confidence level. The upper limit for each mode is determined using the combined likelihood for the two η decay channels with the reconstruction efficiency reduced by 1σ. We vary the signal PDF and the expected ηK^* feed-down in the ηK^0 mode to compute the likelihood as a function of branching fraction; the largest branching fraction that covers 90% of the likelihood area is chosen to be the upper limit.

Significant signals are observed for charged B decays. We investigate their partial rate asymmetries by extracting signal yields separately from the B^+ and B^- samples. Unbinned maximum-likelihood fits are performed independently for the two η decay modes in order to reduce the systematic uncertainties. The same signal and background PDFs as used in the branching fraction measurement are applied. The parameters of the continuum PDF are fixed according to the branching fraction results. Contributions from $B\overline{B}$ backgrounds are required to be equal for the B^+ and B^- samples. Figure 2 shows the $M_{\rm bc}$ and ΔE projections. The A_{CP} results for the two η decay modes are combined assuming that the errors are Gaussian. Systematic errors due to uncertainties in the signal PDF are estimated by varying the peak positions and resolutions. We also check the A_{CP} values after varying the amount of the expected ηK^* feed-down and the reflection background. When determining the systematic error the $B\overline{B}$ contributions are allowed to differ. The largest uncertainty is the asymmetry of the reflection background. A possible detector bias in A_{CP} is studied using $B \to D\pi^+$ decays. The obtained uncertainty is 0.5%. Each A_{CP} deviation is added quadratically to provide the total systematic uncertainty.

In summary, we have observed $B^+ \to \eta\pi^+$ and found evidence for $B^+ \to \eta K^+$; the measured branching fractions and partial rate asymmetries are summarized in Table I. We conclude that the $B^+ \to \eta\pi^+$ branching fraction is larger than that of $B^+ \to \eta K^+$. The measured $B^+ \to \eta\pi^+$ branching fraction is consistent with an earlier result published by the BABAR Collaboration; however, unlike

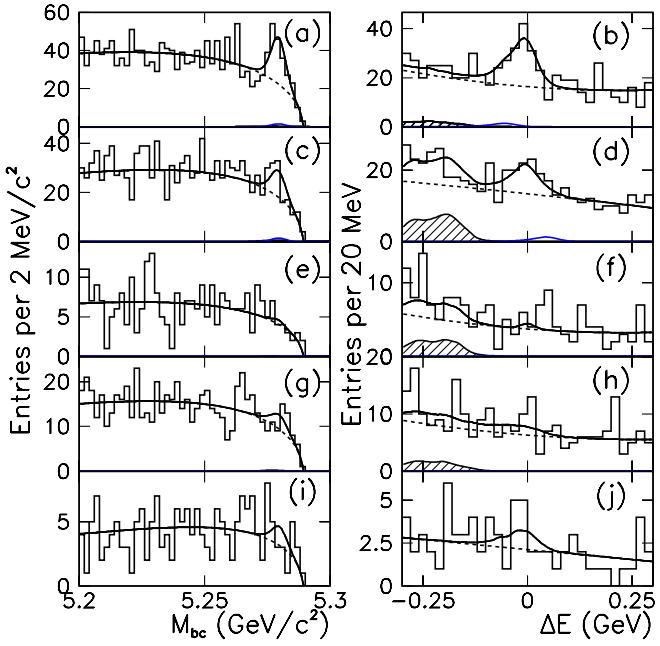

FIG. 1 (color online). $M_{\rm bc}$ and ΔE projections for (a,b) $B^+ \to \eta\pi^+$, (c,d) $B^+ \to \eta K^+$, (e,f) $B^0 \to \eta K^0$, (g,h) $B^0 \to \eta\pi^0$ and (i,j) $B^0 \to \eta\eta$ decays with the $\eta_{\gamma\gamma}$ and $\eta_{3\pi}$ modes combined. Open histograms are data, solid curves are the fit functions, dashed lines show the continuum contributions and shaded histograms are the $\eta K^*/\eta\rho$ contributions. The small contributions around $M_{\rm bc} = 5.28$ GeV$/c^2$ and $\Delta E = \pm 0.05$ GeV in (a)-(d) are the reflection backgrounds from $B^+ \to \eta K^+$ and $B^+ \to \eta\pi^+$.

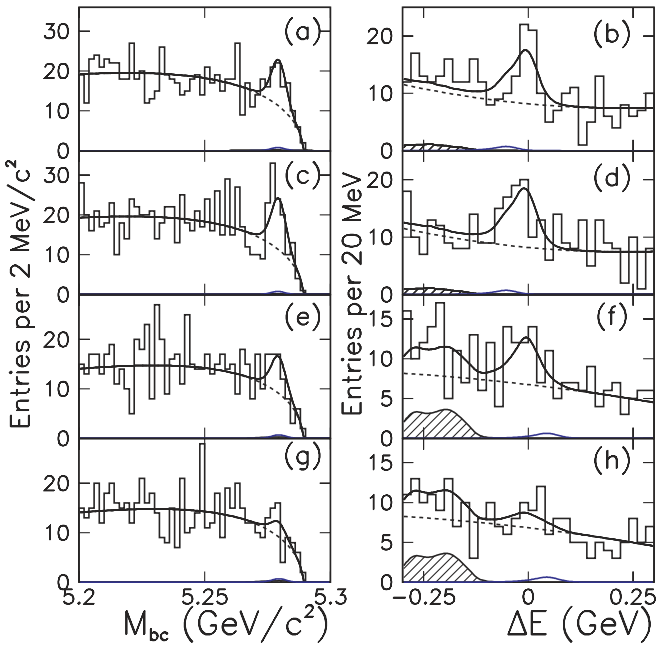

FIG. 2 (color online). $M_{\rm bc}$ and ΔE projections for (a,b) $B^+ \to \eta\pi^+$, (c,d) $B^- \to \eta\pi^-$, (e,f) $B^+ \to \eta K^+$, and (g,h) $B^- \to \eta K^-$ with the $\eta_{\gamma\gamma}$ and $\eta_{3\pi}$ modes combined. Open histograms are data, solid curves are the fit functions, dashed lines show the continuum contributions and shaded histograms are the $\eta K^*/\eta\rho$ contributions. The small contributions near $M_{\rm bc} = 5.28$ GeV$/c^2$ and $\Delta E = \pm 0.05$ GeV are the backgrounds from misidentified $B^+ \to \eta\pi^+$ and $B^+ \to \eta K^+$ (reflections).

the large negative A_{CP} measured by BABAR, the central value in this analysis is small and positive, and is consistent with no asymmetry. For the decay $B^+ \to \eta K^+$, the measured branching fraction is 40% lower than the published result of the BABAR experiment, but they are still consistent within 1.3 σ. It is interesting to note that although the errors are still large, both experiments suggest a large negative A_{CP} value for $B^+ \to \eta K^+$, which is anticipated by some theories [18]. No significant signals are found in neutral $B \to \eta h$ decays and upper limits at the 90% confidence level are given.

We thank the KEKB group for the excellent operation of the accelerator, the KEK Cryogenics group for the efficient operation of the solenoid, and the KEK computer group and the National Institute of Informatics for valuable computing and Super-SINET network support. We acknowledge support from the Ministry of Education, Culture, Sports, Science, and Technology of Japan and the Japan Society for the Promotion of Science; the Australian Research Council and the Australian Department of Education, Science and Training; the National Science Foundation of China under contract No. 10175071; the Department of Science and Technology of India; the BK21 program of the Ministry of Education of Korea and the CHEP SRC program of the Korea Science and Engineering Foundation; the Polish State Committee for Scientific Research under contract No. 2P03B 01324; the Ministry of Science and Technology of the Russian Federation; the Ministry of Education, Science and Sport of the Republic of Slovenia; the National Science Council and the Ministry of Education of Taiwan; and the U. S. Department of Energy.

[1] S. J. Richichi *et al.* (CLEO Collaboration), Phys. Rev. Lett. **85**, 520 (2000).
[2] K. Abe *et al.* (Belle Collaboration), Phys. Lett. B **517**, 309 (2001); B. Aubert *et al.* (BABAR Collaboration), Phys. Rev. Lett. **91**, 161801 (2003).
[3] H. J. Lipkin, Phys. Lett. B **254**, 247 (1991).
[4] M. Bander, D. Silverman, and A. Soni, Phys. Rev. Lett. **43**, 242 (1979); M.-Z. Yang and Y.-D. Yang, Nucl. Phys. **B609**, 469 (2001); M. Beneke and M. Neubert, Nucl. Phys. **B651**, 225 (2003).
[5] Throughout this paper, the inclusion of the charge conjugate mode decay is implied unless otherwise stated.
[6] S. Barshay, D. Rein, and L. M. Sehgal, Phys. Lett. B **259**, 475 (1991); A. S. Dighe, M. Gronau, and J. L. Rosner, Phys. Rev. Lett. **79**, 4333 (1997).
[7] B. Aubert *et al.* (BABAR Collaboration), Phys. Rev. Lett. **92**, 061801 (2004).
[8] Y.-Y. Keum and A. I. Sanda, Phys. Rev. D **67**, 054009 (2003); C.-W. Chiang, M. Gronau, J. L. Rosner, and D. A. Suprun, Phys. Rev. D **70**, 034020 (2004).
[9] S. Kurokawa and E. Kikutani, Nucl. Instrum. Meth.A **499**, 1 (2003), and other papers included in this volume.
[10] A. Abashian *et al.* (Belle Collaboration), Nucl. Instr. Meth. A **479**, 117 (2002).
[11] R. A. Fisher, Ann. Eugenics **7**, 179 (1936).
[12] E. Farhi, Phys. Rev. Lett. **39**, 1587 (1977).
[13] The Fox-Wolfram moments were introduced in G. C. Fox and S. Wolfram, Phys. Rev. Lett. **41**, 1581 (1978); The Fisher discriminant used by Belle, based on modified Fox-Wolfram moments (SFW), is described in K. Abe *et al.* (Belle Collaboration), Phys. Rev. Lett. **87**, 101801 (2001).
[14] R. Ammar *et al.* (CLEO Collaboration), Phys. Rev. Lett. **71**, 674 (1993).
[15] H. Kakuno *et al.* (Belle Collaboration), Nucl. Instr. Meth. A **533**, 516 (2004).
[16] H. Albrecht *et al.* (ARGUS Collaboration), Phys. Lett. B **241**, 278 (1990).
[17] B. Aubert *et al.* (BABAR Collaboration), Phys. Rev. D **70**, 032006 (2004).
[18] C.-W. Chiang, M. Gronau, and J. L. Rosner, Phys. Rev. D **68**, 074012 (2003); S. Barshay and G. Kreyerhoff, Phys. Lett. B **578**, 330, (2004).